Surface & Coatings Technology 392 (2020) 125760

Contents lists available at ScienceDirect

Surface & Coatings Technology

journal homepage: www.elsevier.com/locate/surfcoat

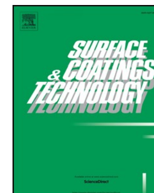

Admittance studies of modification of HgCdTe surface properties with ion implantation and thermal annealing

A.G. Korotaev[a], A.V. Voitsekhovskii[a], I.I. Izhnin[a,b], K.D. Mynbaev[c,d], S.N. Nesmelov[a,*], S.M. Dzyadukh[a], V.S. Varavin[e], S.A. Dvoretsky[a,e], N.N. Mikhailov[e], M.V. Yakushev[e], G.Y. Sidorov[e]

[a] National Research Tomsk State University, 36 Lenin Av., 634050 Tomsk, Russia
[b] Scientific Research Company "Electron-Carat", 202 Stryjska Str., Lviv 79031, Ukraine
[c] Ioffe Institute, 26 Polytechnicheskaya Str., 194021 Saint-Petersburg, Russia
[d] ITMO University, 49 Kronverkskiy Av., 197101 Saint-Petersburg, Russia
[e] A.V. Rzhanov Institute of Semiconductor Physics of SB RAS, 13 Lavrent'ev Av., 630090 Novosibirsk, Russia

ARTICLE INFO

Keywords:
Mercury cadmium telluride
Molecular beam epitaxy
Ion implantation
Thermal annealing
MIS structure
Admittance

ABSTRACT

Metal–insulator–semiconductor (MIS) structures based on HgCdTe were fabricated after various stages of *pn* junction formation using As^+ implantation and activation annealing. The energy of As^+ ions was 200 keV with the fluence of 10^{14} cm^{-2}. Heteroepitaxial HgCdTe films with near-surface graded-gap layers were grown by molecular beam epitaxy (MBE) on silicon substrates. It was shown that the electron concentration in the near-surface semiconductor layer increases after implantation to values of about 10^{17} cm^{-3}, and after implantation and annealing in the near-surface semiconductor layer, a p^+ layer appears with a hole concentration of more than 1.5×10^{18} cm^{-3}. The generation rate of minority charge carriers in the space charge region after implantation is low, which indicates a low defectiveness of the thin near-surface MBE HgCdTe layer. After implantation and annealing, the generation rate increases significantly, which may be due to high defectiveness near the interface between Al_2O_3 and MBE HgCdTe. Dopant profiles were constructed in the near-surface HgCdTe layers after various technological procedures. It was shown that after implantation in films, the dopant concentration increases with distance from the interface to the depth of 0.1 μm.

1. Introduction

The semiconductor solid solution $Hg_{1-x}Cd_xTe$ (HgCdTe) remains the main material for the creation of highly sensitive infrared detectors [1,2] due to its favorable fundamental properties. The band gap of HgCdTe depends on the component composition *x*, which allows one to create intrinsic infrared detectors for various spectral ranges [3]. Currently, hybrid focal plane arrays of HgCdTe-based photodiodes are popular for mid- and long-wavelength infrared ranges (3–5 and 8–12 μm, respectively) [4–6]. Due to the low values of dark currents, much attention is paid to p^+–n photodiodes [6–10], in which the electron-hole transition is usually formed using arsenic ion implantation.

Despite numerous studies, there is still no complete understanding of all the features of the formation of *pn* junctions in graded-gap HgCdTe grown by molecular beam epitaxy (MBE). Therefore, the use of new experimental approaches for studying processes during ion implantation in MBE HgCdTe may be of some interest.

There are known studies on the properties of the implanted material using optical measurements, Rutherford backscattering, electron microscopy [11–14], as well as Hall measurements [11,15]. Hall measurements generally provide information on the integral properties of semiconductor films, so such measurements can be supplemented by the results of studies of the electrical characteristics of metal–insulator–semiconductor (MIS) structures. MIS structures can be made based on HgCdTe MBE films after various technological procedures. The results of measurements of the electrical characteristics of MIS structures are informative when studying the properties of the near-surface layer of HgCdTe, the thickness of which is determined by the thickness of the space charge region (SCR) and usually does not exceed 1 μm.

The aim of the article is to study the properties of the near-surface layer of MBE HgCdTe after various stages of *pn* junction formation by implantation and subsequent thermal annealing using the admittance measurements of test MIS structures.

* Corresponding author.
E-mail addresses: vav43@mail.tsu.ru (A.V. Voitsekhovskii), nesm69@mail.ru (S.N. Nesmelov).

https://doi.org/10.1016/j.surfcoat.2020.125760
Received 8 October 2019; Received in revised form 1 April 2020; Accepted 8 April 2020
Available online 12 April 2020
0257-8972/ © 2020 Elsevier B.V. All rights reserved.

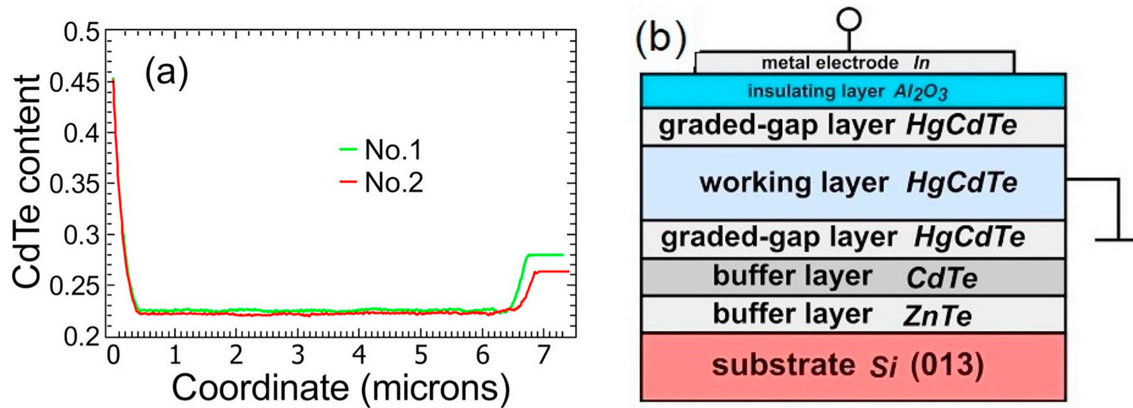

Fig. 1. Distributions of the composition over the thickness for Nos. 1 and 2 films obtained using ellipsometry (a) and the schematic representation of the investigated MIS structures (b).

2. Experimental procedures

HgCdTe films were grown by MBE on silicon substrates at the Institute of Semiconductor Physics of the Siberian Branch of the RAS, Novosibirsk. Two different MBE HgCdTe films (Nos. 1 and 2) were chosen for the investigations. The composition in the working layer was the same for both films ($x = 0.22$). On both sides of the working layer, graded-gap layers with a high CdTe content were formed, the parameters of which were close for both films (Fig. 1(a)). During the growth of the film, they were doped with a donor impurity of indium.

Various technological procedures were carried out with the films, which are necessary to create a *pn* junction. Ion implantation was carried out on an IMC200 setup with As^+ ions with the energies of 200 keV and the fluence of 10^{14} cm^{-2}. After implantation, activation annealing was carried out, which consisted of two stages. The first stage of annealing was carried out in saturated mercury vapor for 2 h at the temperature of 360 °C and was necessary for activation of the introduced arsenic impurity and annihilation of radiation defects. The second stage of annealing was carried out for 24 h at the temperature of 220 °C. This stage made it possible to restore the properties of the base region and anneal the mercury vacancies arising in the first stage. The same annealing of the as-grown films was performed to study the effect of this annealing on the properties of MBE n-HgCdTe.

For the fabrication of MIS structures, the as-grown films (after growing), films after annealing, after ion implantation, and after ion implantation and annealing were chosen. Then MIS structures were formed on the basis of these films by plasma-enhanced atomic layer deposition (PE ALD) of an Al_2O_3 dielectric layer [16–18] with the thickness of about 80 nm and the subsequent formation of indium field electrodes. Fig. 1(b) schematically shows the location of the layers in the fabricated MIS structures.

Admittance dependences were studied using a setup for admittance spectroscopy of nanoheterostructures. This setup includes Agilent E4980A immittance meter, Lake Shore temperature controller and Janis non-optical cryostat. For the reverse direction of the voltage sweep (RVS), the bias voltage was changed from positive values to negative ones, and for the forward direction of the voltage sweep (FVS), from negative to positive ones. The measurements were carried out in the temperature range of 10–300 K at the frequencies of the test signal from 1 to 2000 kHz.

3. Results and discussion

Fig. 2(a) shows the capacitance–voltage (C–V) characteristics of MIS structures No. 1 based on as-grown HgCdTe. It can be seen that at the frequency of 10 kHz, the low-frequency behavior of C–V curves is observed, and at the frequency of 1 MHz, the behavior of the dependences is close to high-frequency. Capacitive dependences exhibit a noticeable hysteresis due to the presence of slow states in the transition layer between the dielectric and the semiconductor. A characteristic feature of hysteresis is the difference in the slopes of the C–V curves in the depletion mode for FVS and RVS [19]. This difference is due to the recharging of slow states in the voltage range corresponding to the section of capacitance change. Fig. 2(b) shows that the C–V characteristics of the MIS structures based on as-grown MBE HgCdTe significantly decreased after annealing. The behavior of capacitive dependences has become more low-frequency, which is clearly visible for the curves measured at the frequency of 200 kHz. Fig. 2(c) shows the C–V curves of the MIS structure based on HgCdTe after implantation. Capacitive dependences show a large hysteresis and high-frequency behavior at all frequencies used (even at the relatively low frequency of 10 kHz). The difference in capacitance of different MIS structures in the accumulation mode is due to the difference in the areas of indium field electrodes. Fig. 2(d) shows that for the C–V curves of the MIS structure based on HgCdTe after implantation and activation annealing, a small hysteresis is characteristic. Capacitive dependences show low-frequency behavior over the entire range of frequencies used (even at the frequency of 1 MHz). The type of C–V characteristics is typical for MIS structures based on a *p*-type semiconductor. Thus, after implantation and activation annealing, the conductivity type of the near-surface MBE HgCdTe layer changed. All the noted features of the C–V characteristics were also observed for structures No. 2.

Fig. 3 shows the changes in some parameters of MIS structures after various technological procedures. The concentration of the majority charge carriers in the near-surface layer of the graded-gap MBE HgCdTe was determined by the minimum capacitance value on the C–V curves. This technique was specially developed for studying the properties of MIS structures based on MBE HgCdTe with a near-surface graded-gap layer [20]. Fig. 3(a) shows that the electron concentrations for the as-grown film and the film after annealing are quite close and amount to (5–7) × 10^{15} cm^{-3} for Nos. 1 and 2. After implantation, the conductivity type of the near-surface layer of the semiconductor has not changed, but the electron concentration increased to about 10^{17} cm^{-3} for both types of films. After implantation and activation annealing, the conductivity type of the MBE HgCdTe near-surface layer changed. The concentration of holes in the near-surface layer of films Nos. 1 and 2 almost reaches 2 × 10^{18} cm^{-3}.

Fig. 3(b) shows the values of the differential resistance of the SCR in the strong inversion mode (R_{SCR}) and the series resistance of the film bulk (R_{bulk}) after various technological procedures. It can be seen that the R_{SCR} value for the films after implantation assumes large values, and the corresponding values for the films after implantation and activation annealing are extremely small. It can be noted that the R_{SCR} value determines the behavior of the C–V characteristics and depends on the

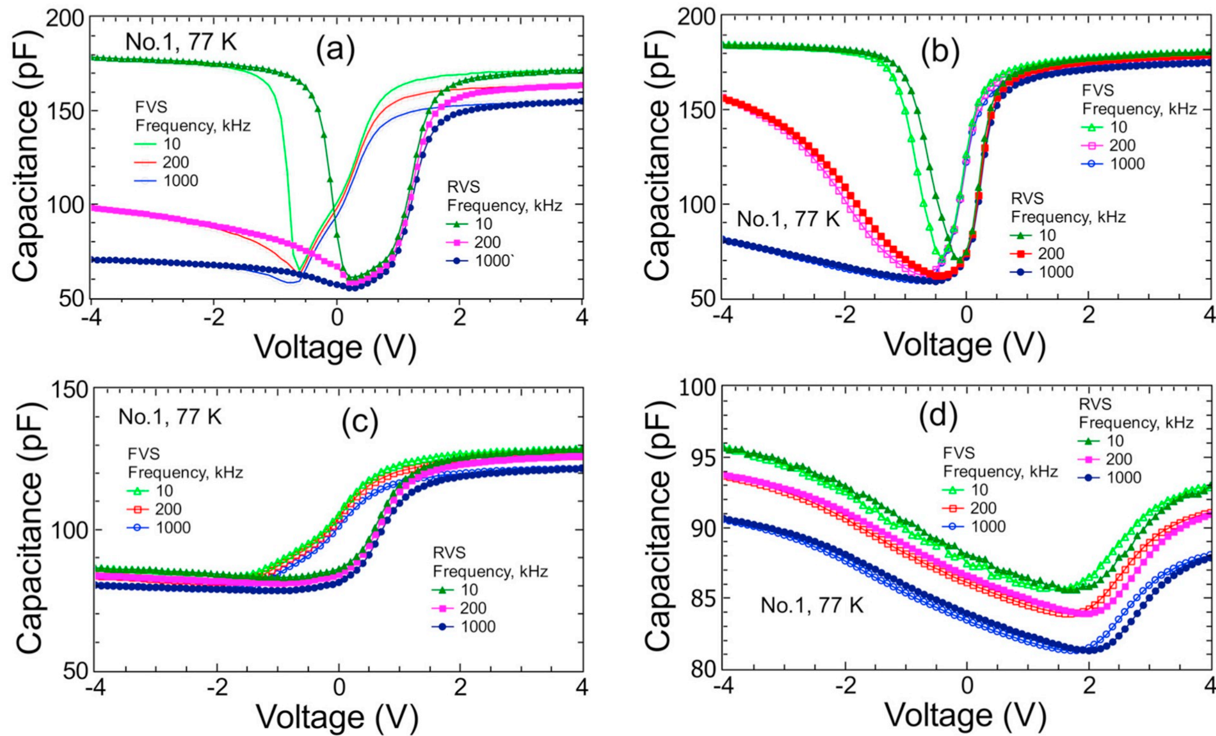

Fig. 2. C–V curves of MIS structures based on MBE HgCdTe films after growing (a), after activation annealing (b), after ion implantation (c), and after implantation and activation annealing (d).

generation rate of minority charge carriers in the near-surface semiconductor region. This generation rate is determined by the presence of defects through which generation and recombination in the SCR can pass. Therefore, it can be assumed that the defect concentration in the near-surface MBE HgCdTe layer is low after implantation, but increases significantly after implantation and activation annealing. An increase in the generation rate of minority charge carriers after implantation and annealing can be associated with an increase in the role of defects located near the interface. With an increase in the dopant concentration, the SCR width decreases and the role of generation near the interface increases. The values of the series resistance of the film bulk are not the same after various technological procedures (Fig. 3(b)), but changes in this parameter are less pronounced. It should be noted that the series resistance of the bulk may vary slightly due to the peculiarities of the relative position of the front and backward electrodes for different MIS structures.

Significant hysteresis is typical for MIS structures based on MBE HgCdTe with near-surface graded-gap layers using an Al_2O_3 dielectric [19]. This hysteresis distorts the C–V curves in the depletion mode, which makes it difficult to determine, for example, the distribution of the concentration of the dopant in the surface layer of the semiconductor by the slope of the $C^{-2}(V)$ dependence in depletion [21]. To exclude the effect of slow-state recharging on the C–V characteristics of MIS structures based on MBE HgCdTe, we used a «narrow swing» technique for studying electrical characteristics with a complex form of voltage sweep [19]. This technique was previously proposed for the study of MIS structures based on InSb [22,23]. Fig. 4 shows the distribution of dopant concentration over the thickness of the near-surface layer of MBE HgCdTe films after various technological procedures. The apparent increase in the concentration of the dopant at small and large distances from the interface is due to a violation of the depletion approximation [24–26]. Dopant profiles are in good agreement with the dopant concentration values found from the minimum capacitance values on C–V characteristics. Comparison of Fig. 3(a) and Fig. 4 shows that the minimum value of capacitance determines the dopant concentration at the interface between the SCR and the quasi-neutral semiconductor bulk. Fig. 4 shows that after implantation in the films, the dopant concentration increases with the distance from the interface

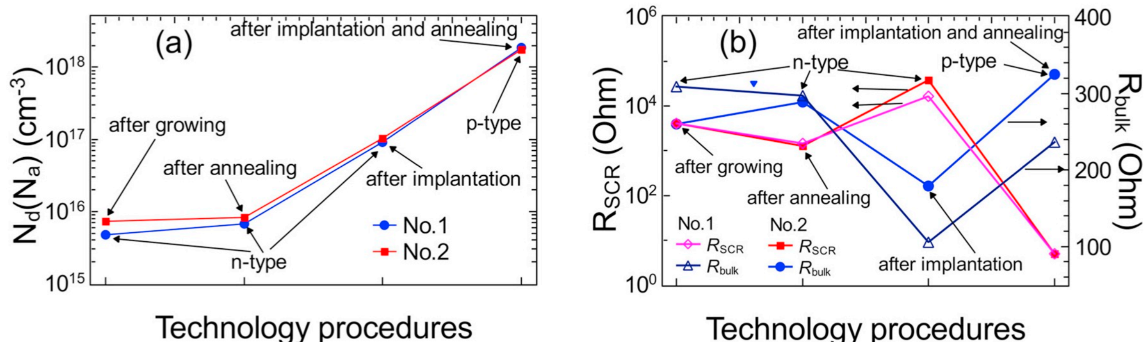

Fig. 3. The values of the MIS structure parameters after various technological procedures: the dopant concentration (a) and the SCR resistance and the series resistance of the MBE HgCdTe film bulk (b).

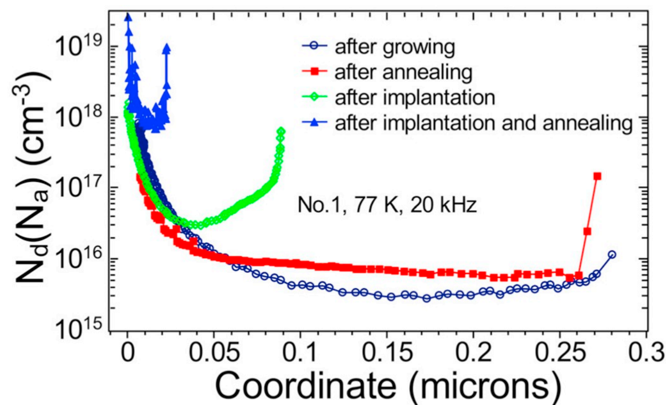

Fig. 4. Distributions of dopant concentration over the thickness of the surface layer of MBE HgCdTe film after various technological procedures, constructed using the «narrow swing» technique.

between the insulator and the semiconductor to the depth of about 0.1 μm.

4. Conclusions

Thus, the electrical characteristics of MIS structures based on graded-gap MBE HgCdTe films were studied after various technological procedures used to form the *pn* junction using ion implantation and activation annealing. It was shown that the properties of as-grown *n*-HgCdTe films and films after growing and activation annealing do not differ very much. After ion implantation, the high electron concentration (about 10^{17} cm^{-3}) is observed in the near-surface layer of films, and high values of differential resistance are measured, which indicates a low defectiveness of the layer up to the depth of 0.1 μm. After implantation in MBE HgCdTe films and annealing, the conductivity type of the near-surface semiconductor layer changes, in which the high concentration of holes is observed (almost up to 2×10^{18} cm^{-3}). For films after implantation and annealing, very small values of the differential SCR resistance are observed, which may be due to the large contribution of the generation of minority charge carriers in the transition layer between the insulator and semiconductor. It was found that after activation annealing, the hysteresis of the C–V characteristics decreases, which indicates a decrease in the density of slow states in the transition layer between the MBE HgCdTe and the Al_2O_3. A method for determining dopant profiles in the near-surface layer of MBE HgCdTe is proposed, and profiles are constructed after various technological procedures. It was shown that after implantation in films, the dopant concentration increases with distance from the interface to the depth of 0.1 μm. The admittance measurements of MIS structures formed on the basis of MBE HgCdTe films after various technological procedures are shown to be informative.

CRediT authorship contribution statement

A.G. Korotaev:Project administration, Visualization.**A.V. Voitsekhovskii:**Conceptualization, Supervision, Funding acquisition, Writing - review & editing.**I.I. Izhnin**:Methodology.**K.D. Mynbaev**:Validation.**S.N. Nesmelov**:Investigation, Writing - original draft, Writing - review & editing.**S.M. Dzyadukh**:Investigation, Software, Data curation.**V.S. Varavin**:Resources.**S.A. Dvoretsky**:Resources.**N.N. Mikhailov**:Resources.**M.V. Yakushev**:Res ources.**G.Y. Sidorov**:Resources.

Declaration of competing interest

The authors declare that they have no known competing financial interests or personal relationships that could have appeared to influence the work reported in this paper.

Acknowledgements

This study was supported by "The Tomsk State University competitiveness improvement programme" (Project No. 8.2.04.2018).

References

[1] A. Rogalski, P. Martyniuk, M. Kopytko, Challenges of small-pixel infrared detectors: a review, Rep. Prog. Phys. 79 (2016) 046501, , https://doi.org/10.1088/0034-4885/79/4/046501.
[2] W. Lei, J. Antoszewski, L. Faraone, Progress, challenges, and opportunities for HgCdTe infrared materials and detectors, Appl. Phys. Rev. 2 (2015) 041303, , https://doi.org/10.1063/1.4936577.
[3] L. Mollard, G. Bourgeois, C. Lobre, S. Gout, S. Viollet-Bosson, N. Baier, G. Destefanis, O. Gravrand, J.P. Barnes, F. Milesi, A. Kerlain, L. Rubaldo, A. Manissadjian, p-on-n HgCdTe infrared focal-plane arrays: from short-wave to very-long-wave infrared, J. Electron. Mater. 43 (2014) 802–807, https://doi.org/10.1007/s11664-013-2809-3.
[4] W.E. Tennant, D.J. Gulbransen, A. Roll, M. Carmody, D. Edwall, A. Julius, P. Dreiske, A. Chen, W. McLevige, S. Freeman, D. Lee, D.E. Cooper, E. Piquette, Small-pitch HgCdTe photodetectors, J. Electron. Mater. 43 (2014) 3041–3046, https://doi.org/10.1007/s11664-014-3192-4.
[5] W. Qiu, W. Hu, C. Lin, X. Chen, W. Lu, Surface leakage current in 12.5 μm long-wavelength HgCdTe infrared photodiode arrays, Opt. Lett. 41 (2016) 828–831, https://doi.org/10.1364/OL.41.000828.
[6] A. Kerlain, A. Brunner, D. Sam-Giao, N. Pére-Laperne, L. Rubaldo, V. Destefanis, F. Rochette, C. Cervera, Mid-wave HgCdTe FPA based on P on N technology: hot recent developments. NETD: dark current and 1/f noise considerations, J. Electron. Mater. 45 (2016) 4557–4562, https://doi.org/10.1007/s11664-016-4506-5.
[7] J.H. Park, J. Pepping, A. Mukhortova, S. Ketharanathan, R. Kodama, J. Zhao, D. Hansel, S. Velicu, F. Aqariden, Development of high-performance eSWIR HgCdTe-based focal-plane arrays on silicon substrates, J. Electron. Mater. 45 (2016) 4620–4625, https://doi.org/10.1007/s11664-016-4717-9.
[8] L. Mollard, G. Destefanis, G. Bourgeois, A. Ferron, N. Baier, O. Gravrand, J.P. Barnes, A.M. Papon, F. Milesi, A. Kerlain, L. Rubaldo, Status of *p*-on-*n* arsenic-implanted HgCdTe technologies, J. Electron. Mater. 40 (2011) 1830, https://doi.org/10.1007/s11664-011-1692-z.
[9] L. Mollard, G. Destefanis, N. Baier, J. Rothman, P. Ballet, J.P. Zanatta, M. Tchagaspanian, A.M. Papon, G. Bourgeois, J.P. Barnes, C. Pautet, P. Fougeres, Planar *p*-on-*n* HgCdTe FPAs by arsenic ion implantation, J. Electron. Mater. 38 (2009) 1805, https://doi.org/10.1007/s11664-009-0829-9.
[10] C.Z. Shi, C. Lin, Y.F. Wei, L. Chen, M. Zhu, Barrier layer induced channeling effect of As ion implantation in HgCdTe and its influences on electrical properties of *p*–*n* junctions, Appl. Opt. 55 (2016) D101, https://doi.org/10.1364/AO.55.00D101.
[11] I.I. Izhnin, A.V. Voitsekhovsky, A.G. Korotaev, O.I. Fitsych, A.Y. Bonchyk, H.V. Savytskyy, K.D. Mynbaev, V.S. Varavin, S.A. Dvoretsky, N.N. Mikhailov, M.V. Yakushev, R. Jakiela, Optical and electrical studies of arsenic-implanted HgCdTe films grown with molecular beam epitaxy on GaAs and Si substrates, Infrared Phys. Technol. 81 (2017) 52–58, https://doi.org/10.1016/j.infrared.2016.12.006.
[12] C. Lobre, D. Jalabert, I. Vickridge, E. Briand, D. Benzeggouta, L. Mollard, P.H. Jouneau, P. Ballet, Quantitative damage depth profiles in arsenic implanted HgCdTe, Nucl. Instrum. Methods Phys. Res. Sect. B 313 (2013) 76–80, https://doi.org/10.1016/j.nimb.2013.07.019.
[13] C. Lobre, P.H. Jouneau, L. Mollard, P. Ballet, Characterization of the microstructure of HgCdTe with p-type doping, J. Electron. Mater. 43 (2014) 2908–2914, https://doi.org/10.1007/s11664-014-3147-9.
[14] S. Simingalam, P. Wijewarnasuriya, M.V. Rao, Thermal cycle annealing and its application to arsenic-ion implanted HgCdTe, 2014 20th International Conference on Ion Implantation Technology (IIT), IEEE, 2014, pp. 1–4, , https://doi.org/10.1109/IIT.2014.6940053.
[15] I.I. Izhnin, I.I. Syvorotka, O.I. Fitsych, V.S. Varavin, S.A. Dvoretsky, D.V. Marin, N.N. Mikhailov, V.G. Remesnik, M.V. Yakushev, K.D. Mynbaev, A.V. Voitsekhovsky, A.G. Korotaev, Electrical profiling of arsenic-implanted HgCdTe films performed with discrete mobility spectrum analysis, Semicond. Sci. Technol. 34 (2019) 035009, , https://doi.org/10.1088/1361-6641/aafc6a.
[16] R. Fu, J. Pattison, Advanced thin conformal Al_2O_3 films for high aspect ratio mercury cadmium telluride sensors, Opt. Eng. 51 (2012) 104003, , https://doi.org/10.1117/1.OE.51.10.104003.
[17] P. Zhang, Z.H. Ye, C.H. Sun, Y.Y. Chen, T.N. Zhang, X. Chen, C. Lin, R.-J. Ding, L. He, Passivation effect of atomic layer deposition of Al_2O_3 film on HgCdTe infrared detectors, J. Electron. Mater. 45 (2016) 4716–4720, https://doi.org/10.1007/s11664-016-4686-z.
[18] P. Zhang, C.H. Sun, Y. Zhang, X. Chen, K. He, Y.Y. Chen, Z.H. Ye, Thermal stability of atomic layer deposition Al_2O_3 film on HgCdTe, Proc. SPIE 9451 (2015) 94512A, https://doi.org/10.1117/12.2180414.
[19] A.V. Voitsekhovskii, S.N. Nesmelov, S.M. Dzyadukh, V.S. Varavin, S.A. Dvoretsky, N.N. Mikhailov, M.V. Yakushev, G.Y. Sidorov, Electrical characterization of insulator-semiconductor systems based on graded band gap MBE HgCdTe with atomic layer deposited Al_2O_3 films for infrared detector passivation, Vacuum 158 (2018)

136–140, https://doi.org/10.1016/j.vacuum.2018.09.054.
[20] A.V. Voitsekhovskii, S.N. Nesmelov, S.M. Dzyadukh, Admittance measurements in the temperature range $(8-77)$ K for characterization of MIS structures based on MBE *n*-$Hg_{0.78}Cd_{0.22}Te$ with and without graded-gap layers, J. Phys. Chem. Sol. 102 (2017) 42–48, https://doi.org/10.1016/j.jpcs.2016.10.015.
[21] W. Van Gelder, E.H. Nicollian, Silicon impurity distribution as revealed by pulsed MOS C-V measurements, J. Electrochem. Soc. 118 (1971) 138–141, https://doi.org/10.1149/1.2407927.
[22] T. Nakagawa, H. Fujisada, Method of separating hysteresis effects from MIS capacitance measurements, Appl. Phys. Lett. 31 (1977) 348–350, https://doi.org/10.1063/1.89695.
[23] T. Nakagawa, H. Fujisada, Method for evaluation of hysteretic interface properties and their application to anodized InSb MIS diodes, IEE Proc. I (Solid-State Elect. Dev.) 131 (1984) 51–55, https://doi.org/10.1049/ip-i-1.1984.0015.
[24] J.R. Brews, Correcting interface-state errors in MOS doping profile determinations, J. Appl. Phys. 44 (1973) 3228–3231, https://doi.org/10.1063/1.1662738.
[25] A.R. LeBlanc, D.D. Kleppinger, J.P. Walsh, A limitation of the pulsed capacitance technique of measuring impurity profiles, J. Electrochem. Soc. 119 (1972) 1068, https://doi.org/10.1149/1.2404400.
[26] S.T. Lin, J. Reuter, The complete doping profile using MOS CV technique, Solid State Electron. 26 (1983) 343–351, https://doi.org/10.1016/0038-1101(83)90134-X.